Pore cross-talk in colloidal filtration

Olivier Liot, Akash Singh, Patrice Bacchin, Paul Duru, Jeffrey Morris, Pierre Joseph

Pore cross-talk in colloidal filtration

Olivier Liot,* Akash Singh, Patrice Bacchin,† Paul Duru,‡ Jeffrey F. Morris,§ and Pierre Joseph¶
LAAS-CNRS, Université de Toulouse, CNRS, Toulouse, France
(Dated: November 29, 2017)

Blockage of pores by particles is found in numerous industrial and natural processes, including filtration and oil extraction. We present experimental results of filtration through a linear array of ten channels with one dimension which is sub-micron. These silicon-glass nanoslits serve as model pores, through which a dilute dispersion of Brownian polystyrene spheres flows. The clog growth rate at fixed differential pressure is shown to systematically increase with the number of saturated (entirely clogged) pores, indicating that there is an interaction or "cross-talk" between the pores. This observation is interpreted using a model proposed here, based on the concept that the residual permeability allows a clog to act as a filter. A clogged pore is thus the source of a local increase of particle concentration adjacent to the pore, which then diffuses towards other pores. This phenomenon, evidenced and modelled here in one dimension, should be at play in two-dimensional membranes.

* Fédération FERMaT, INP Toulouse; olivier.liot@laas.fr
† Laboratoire de Génie Chimique, Université de Toulouse, CNRS, Toulouse, France
‡ Institut de Mécanique des Fluides, IMFT, Université de Toulouse, CNRS - Toulouse, France
§ Levich Institute and Chemical Engineering, CUNY City College of New York, USA
¶ pierre.joseph@laas.fr

Introduction

A colloidal suspension flowing through a pore network often results in fouling or clogging. In both industrial (oil recovery [1], inkjet printing [2], filtration), biological (artery diseases [3], detection of cells [**?**]) and natural (water infiltration in soils [4], precipitation inside rocks [5]) processes, the phenomenon of particle accumulation is involved. At the pore scale, recent improvements in visualization of suspended particles in model pores has led to new insight into the physical parameters at play in particle capture and clogging in pores [6]. There are several different clogging mechanisms. Size exclusion or sieving occurs when particles block a pore smaller than their diameter. If the pore size is larger than the particle, clogging can occur by two routes, either through particles forming an arch at the entrance of the pore or progressively adhering to walls and other previously deposited particles. In the latter case, particle aggregates can appear and block the pore [7]. During the last decade, following the early study of Wyss *et al.* [8] which described clogging of pores by smaller particles, a number of studies have focused on determining the pore-scale mechanisms involved in this form of pore blockage (e.g. [9–14]). Other studies have proposed explanations of clogging using transition-state theory [15] or by relating it to jamming phenomena [16].

Prior to the advent of pore-scale investigations, which have been greatly facilitated by microfluidic technology, numerous studies were made at a more macroscopic membrane scale, where the usual focus was on the "filtration cake" [17–20]. Since a typical filtration membrane consists of a large number of closely-spaced pores, clog formation at one pore could affect its neighbours, and hence the macroscopic behavior of the membrane in a filtration process. Considered in this way, there is a notable lack of information related to clog formation at the pore scale, with connection to the membrane scale by consideration of interactions between pores. In this work, we address this gap of knowledge at an intermediate scale, by considering in detail the time evolution of the clog formation process at pore scale, in a short one-dimensional (1-D) array of pores. We describe the interaction between pores as "cross-talk". While one recent paper [15] shows that a filtration cake can overhang neighbouring pores and influence the clog formation, there is, to our knowledge, no direct analysis of the pore cross-talk phenomenon. Yet it could have a dramatic impact on the understanding of filtration process of suspensions at macroscale, such as possible preferential locations of cake formation.

In this work, we present observations of cross-talk when a Brownian suspension flow through a simple 1-D micro-filtration device. The flow is driven by a fixed pressure difference, not a fixed flow rate, and this is a key point of our study. We measure a clogging growth rate as a function of the number of already clogged pores and we propose a model based on a local increase of colloid concentration close to clogged pores to explain the observations. This model, developed for our 1-D pore array, could be extended to 2-D membranes, taking into account the spatial pore distribution.

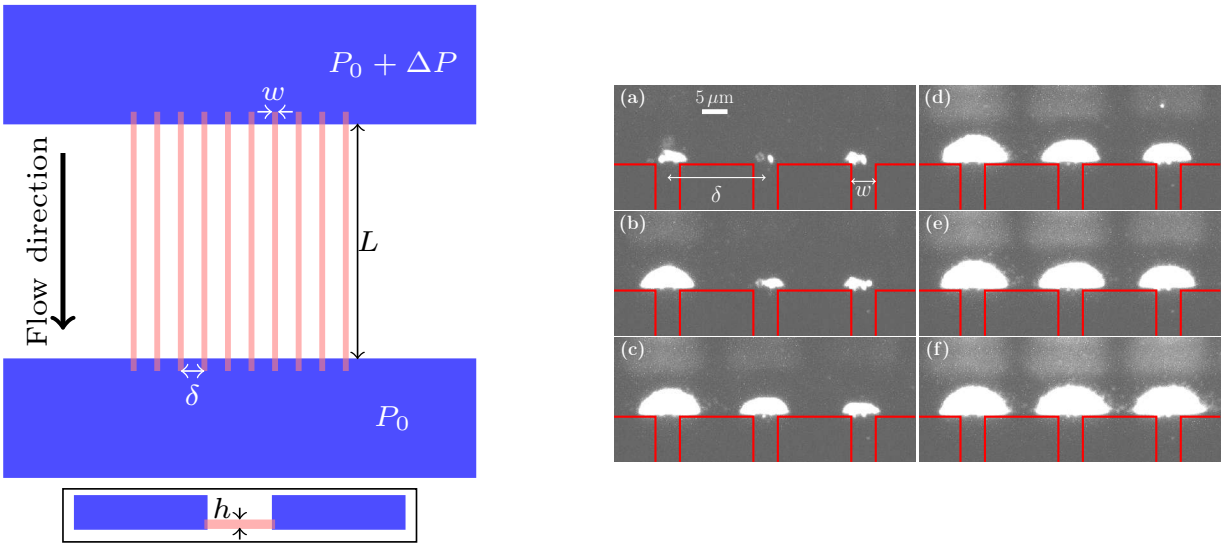

Figure 1. **Sketch of the model pores and micrograph of some clogs.** Left: top view of the chip design with zoom on nanoslits. Microchannels are represented in blue, nanoslits in red. Inset: side view of the nanoslits (not to scale). Right: image of the development of three adjacent clogs at the entrance of pores. Red lines delimit the nanoslits. For (a) to (f) the corresponding times are t=1333, 2000, 2666, 3000, 3333, 4000 s.

Experimental method

Ten nanoslits of width $w = 5\,\mu$m, length $L = 50\,\mu$m, depth $h = 830$ nm, and center-to-center spacing $\delta = 20\ \mu$m are etched in silicon. These nanoslits connect much larger inlet and outlet microchannels. The device is covered with a $170\,\mu$m-thick borosilicate glass plate. The design is presented in Figure 1 (left). As shown in the box at the bottom of Figure 1 (left), the nanoslits connect corners of the cross-section of the microchannels. The channels are filled with a suspension of $d_p = 250$ nm diameter polystyrene particles (density 1.05 g.cm^{-3}). The particles are carboxylate-modified. The input volume fraction of the suspension is $\phi_0 = 3.8 \times 10^{-5}$. Particles are dispersed either in a solution of monovalent phosphate buffered saline (PBS) diluted to anionic strength of $I = 3$ mM, or in ultrapure water ($I \approx 2 \times 10^{-4}$ mM). Addition of salt does not imply formation of particle aggregates. The zeta potentials are measured by laser Doppler elcetrophoresis. We obtain $\zeta_p = -69$ mV (pH = 7.5) and $\zeta_p = -49$ mV (pH = 7.0) respectively. A pressure difference of $\Delta P = 20$ mbar is applied across the length of the nanoslits using a controller device (sensitivity of 0.02 mbar). Experiments are made in dead-end and slow crossflow filtration (with velocity 0 to $9\,\mu$m/s at 2 μm from the entrance of the pores).

The clogging dynamics are observed using wide field fluorescence microscopy with a 40×, 1.4 numerical aperture objective. Since the characteristic time for clogging is found to be about one hour we acquire images of the clog growth process at a frequency of 90 frames per minute. Figure 1 (right) shows an example of the development of three adjacent clogs. The contour of the aggregated particle mass is detected using custom *Python* scripts. From this contour analysis, we are able to determine the projected area of each clog in the field of view.

Experimental results

Figure 2 shows an example of the time evolution of the area of aggregated particles at each of the pore entrances in a single microfluidic chip for $I = 3$ mM. We observe (for example on the black curve) that there is first a slow growth, which corresponds to a progressive accumulation at the given pore entrance, as particles stick to the walls and to one another. This first stage of the clogging dynamics ends when the clog extends fully across the pore entrance. Then, we observe a more rapid, quasi-linear growth up to a saturation level. This saturation is hypothesized to result from a balance between drag forces (note that the flow rate through a pore decreases when the clog grows, leading to a decrease of the drag force exerted on the particles) and Brownian diffusion, corrected for inter-particle repulsive interactions. We observe that when a clog begins its rapid growth after other pores have reached saturation, the growth rate is larger (e.g. compare the green and black curves). We quantitatively define the growth rate (with dimensions of area/time) as the average of the derivative of the measured area with time in the zone where its evolution is linear, see Figure 2. A Gaussian filter [21] is used to remove the measurement noise before averaging.

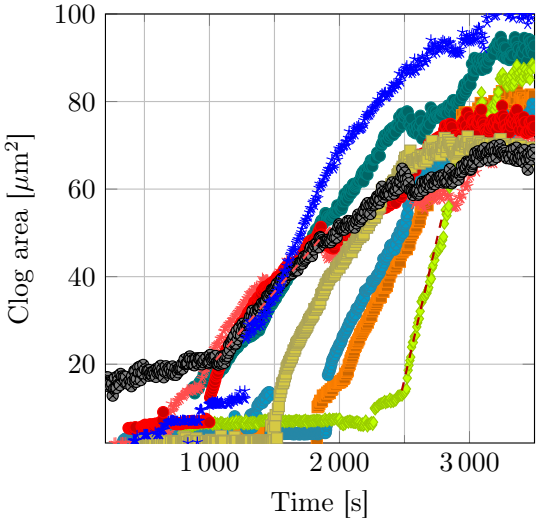

Figure 2. **Time evolution of the clog area during a single acquisition for $I = 3$ mM.** The aggregates formed at nine pore entrances are shown. Drawn lines highlight the zone where clog growth rate is estimated.

We made eight acquisitions for each ionic strength. We define the mean growth rate when N pores are saturated (the clog size reached a saturation) as v_N^*. We have $N \in [0, N_{tot} - 1]$ where N_{tot} is the total number of pores. To combine the different acquisitions, we plot on Figure 3 the ratio v_N^*/v_0^* as a function of N. We observe a clear increase of this ratio when the number of saturated pores increases, from $v_N^*/v_0^* = 1$ for $N = 0$ to $v_N^*/v_0^* \approx 3$ for

$N = 9$. Although the points at low ionic strength appear to be slightly higher than those for lower ionic strength, the difference remains within the error bars. To explain the observed increase of v_N^*/v_0^* with N, we propose a simple model which could be applied to different membrane configurations.

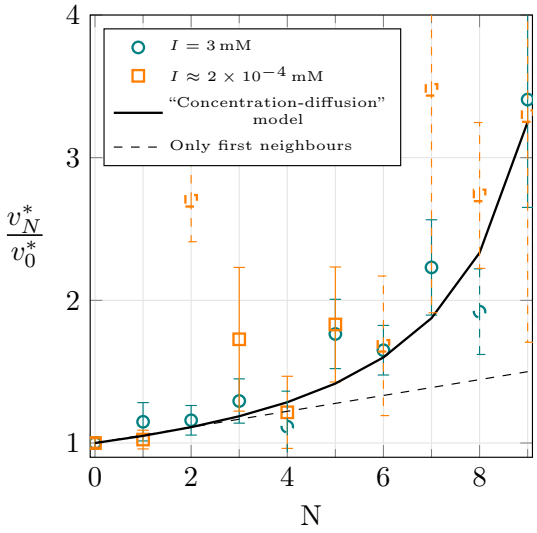

Figure 3. v_N^*/v_0^* **ratio versus** N **for two ionic strengths.** The error bars are related to statistical uncertainty (standard deviation over root square of the number of events); dashed points are low statistic points (less than three events). The solid line represents the equation (4). The dashed line represents the case where only the first neighbour in each direction is accounted in $\langle \aleph \rangle_N$.

"Concentration-diffusion" model

The model we propose is valid only for a fixed pressure drop. In the case of a fixed flow rate, no saturation of the clog size is observed and particles continue to accumulated indefinitely [15]. In our case, an increase of the hydraulic resistance of the saturated pores takes place. Because the Reynolds number is small, $Re = Uh/\nu = O(10^{-3})$, where U is the typical velocity in the nanoslits and ν the kinematic viscosity of the fluid, we estimate the hydraulic resistance using the Blake-Kozeny equation [22],

$$R_h^{clog} = \frac{150\,\ell\eta(1-\varepsilon)^2}{whd_p\varepsilon^3}, \tag{1}$$

where ε represents the clog porosity, η the fluid dynamic viscosity , and ℓ a typical length of the clog. To estimate ℓ, we consider that, because they form in a corner, the clogs are roughly quarter-spheres, and assume that the radius of the clog corresponds to ℓ. Since we know the projected area at saturation, we obtain $\ell \sim 7\mu$m. The porosity can be estimated using a previous study [20], which shows that for pH = 6 (close to that in the present study), and for a small filtration cake of colloids, the porosity can reach $\varepsilon = 0.83$. With these parameters, the hydraulic resistance estimate is $R_h^{clog} = 2 \times 10^{17}$ kg.m^{-4}.s^{-1}. The hydraulic resistance of the rectangular pore is very similar: $R_h^{slit} = 2.3 \times 10^{17}$ kg.m^{-4}.s^{-1} [23]. The resulting flow rate Q_s through a saturated pore will be about one-half of that in an open, or "free", pore (Q_f).

A saturated clog acts as a filter, as there is still fluid passing through. The main idea of the present model is that the particles driven by this permeation flow close to a clogged pore will be "redistributed" by Brownian diffusion along the membrane surface to finally flow through opened pores. The typical time scale t^* between two successive pore clogging events is about 100 s (see Figure 2). The diffusion coefficient of the particles at ambient temperature is $D = 1.7 \times 10^{-12}$ m^2.s^{-1} [24]. Their typical displacement during this time interval in one direction is $\Delta x = \sqrt{2Dt^*} = 18$ μm. Therefore, particle diffusive redistribution is expected to be a relevant mechanism in the present experiments. Note we did not observe noticeable differences between results obtained in dead-end and slow cross-flow filtration, probably because close to the nanochannels entrance, crossflow is slow enough and diffusion dominates.

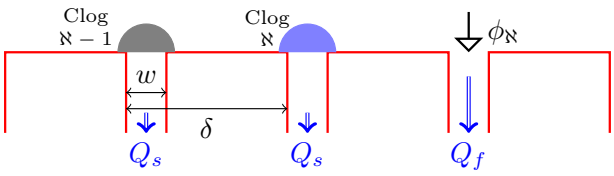

Figure 4. **Sketch of the situation with two saturated pores neighbouring a free pore (therefore, $\aleph = 2$).** Blue double arrows show the flow rate through the pores; black, open triangle arrow represents the particle concentration flux in the free pore.

We propose a stationary "concentration-diffusion" model to estimate the influence of the diffusively-transported particles on clog growth rate. Let us assume that a free pore has $\aleph$ successive neighbouring saturated pores, including left and right directions. Figure 4 sketches the physical configuration in the case $\aleph = 2$ with the two clogs on the left side of the considered free pore. A newly saturated pore acts as a source of particles diffusing in both directions away from the clog, toward the closest free pores. There, the advection process through the pore is much stronger than the diffusive transport. Indeed, a Péclet number which compares advection to diffusion at the particle length scale, is given by $Pe = 6\,\pi\eta d_p^2 U/k_B T$, with T the temperature, U the mean velocity in the nanoslits and k_B the Boltzmann constant. We have $Pe \approx 600$ before start of clogging. Consequently, all the particles redistributed from a saturated pore will be "sucked down" by the first free pores (on both sides of the saturated pore), i.e. will flow through these pores. As a result, the effective concentration of the suspension flowing through a free pore will be simply

$$\phi_\aleph = \phi_0 \left(1 + \aleph \frac{Q_s}{2\,Q_f}\right), \tag{2}$$

each neighbouring clogged pore contributing equally to $\phi_\aleph$ in the present model. However, the variable $\aleph$ is not easily available: it is specific to each free pore, depending on its environment which changes with time, and it depends on the configuration of free and saturated pores. Thereby, this problem has a statistical facet. When N pores out of N_{tot} are saturated, the effective concentration of the suspension flowing in a given opened pore, averaged over all opened-clogged pores configurations is defined as:

$$\langle \phi_\aleph \rangle_N = \phi_0 \left(1 + \langle \aleph \rangle_N \frac{Q_s}{2\,Q_f}\right), \tag{3}$$

where $\langle \aleph \rangle_N$ is the average number of neighbouring saturated pores adjacent to free pores. The clog growth rate is linked to the particle concentration in the pore: $v_N^* \propto \langle \phi_\aleph \rangle_N Q_f$ [8]. Finally, the ratio of clog growth rate with N clogged pores to clog growth rate with no clogged pore can be written as:

$$\frac{v_N^*}{v_0^*} = 1 + \langle \aleph \rangle_N \frac{Q_s}{2\,Q_f}, \tag{4}$$

with $\langle \aleph \rangle_N$ computed using a tree diagram approach (see Supplementary Materials).

Discussion and conclusion

The result of the model given by eq. 4 is plotted (solid line) in Figure 3. It is in very good agreement with the experimental data. Although there is some dispersion, especially for points with low statistical support, the global trend is well captured for both values of the ionic strength. This model does not contain free parameters: $\langle \aleph \rangle_N$ is computed numerically and the only physical parameter used in the model can be directly computed (Q_s). A key point, observed experimentally and well predicted by the model, is that the cross-talk between pores becomes more and more important as N increases. The clogging of a free pore will be influenced by a distant, saturated pore if there are only saturated pores between them. To support this point, Figure 3 shows in dashed line the results of the model obtained considering only the first adjacent neighbour in each direction to compute $\langle \aleph \rangle_N$. For $N < 3$, the average number of successive neighbouring saturated pores is similar to the average number of immediate neighbours. But for higher N, the experimental data are several times higher than this simplified model, which highlights the "long-range" cross-talk between pores captured in the full model (solid line). This effect is expected to depend on the Péclet number. For smaller Péclet numbers, one could expect a more spatially-extended diffusive influence of the particle filtration at a saturated pore. The model could be improved so as to explicitly introduce a Péclet number dependence, but in realistic filtration process this number should remain large compared to 1 and the present model

should apply. Another important quantity for the model is the flow rate Q_s through a saturated pore. It depends on the clog saturated size and internal structure, which both results from a balance between drag force and repulsive interactions between the Brownian particles. Dense clogs with low permeability will induce low Q_s and thus low particle redistribution and weak cross-talk.

To sum-up and conclude, we have directly imaged a filtration process of Brownian nanoparticles in nanoslit entrances at fixed pressure drop. The observation of cross-talk between pores, with an increase of clog growth rate with the number of saturated pores, is the central point of this paper. A way to enhance this phenomenon could be to increase the Brownian diffusion using less viscous fluids or smaller colloids. The cross-talk between pores could have impact on the understanding of membrane fouling dynamics. The model we developed here could be extended to different geometries, particularly 2-D membranes. The pore geometry and distribution on the membrane, and the clog permeability, are the only parameters necessary to estimate the cross-talk between pores. It would be interesting to make similar measurements on 2-D membranes with different pore lattices (e.g., random, square, or hexagonal) and compare with the predictions of the "concentration-diffusion" model in such configurations.

Acknowledgements

We acknowledge the Fédération FERMaT and University of Toulouse (Project NEMESIS) for funding these researches. O. Liot warmly acknowledge M. Socol for his chip microfabrication and experimental help. This work was partly supported by LAAS-CNRS micro and nanotechnologies platform member of the French RENATECH network.

Author contribution

O.L. and A.S. performed experiments and analysis. O.L. developed the model with P.D.. P.J. and O.L. fabricated the microfluidic chips and assembled the experimental device. J.F.M. led the scientific project development within the context of the NEMESIS Chair d'Attractivité at University of Toulouse. O.L. led the manuscript writing, in which P.B., P.D., J.F.M. and P.J. took part.

Competing financial interests

Authors have no competing financial interests.

[1] M. Tavakkoli, M. R. Grimes, X. Liu, C. K. Garcia, S. C. Correa, Q. J. Cox, and F. M. Vargas, "Indirect Method: A Novel Technique for Experimental Determination of Asphaltene Precipitation," Energy & Fuels **29**, 2890–2900 (2015).

[2] S. B. Fuller, E. J. Wilhelm, and J. M. Jacobson, "Ink-jet printed nanoparticle microelectromechanical systems," Journal of Microelectromechanical systems **11**, 54–60 (2002).

[3] M. B. Rothberg, "Coronary Artery Disease as Clogged Pipes: A Misconceptual Model," Circulation: Cardiovascular Quality and Outcomes **6**, 129–132 (2013).

[4] W. Zhang, X. Tang, N. Weisbrod, and Z. Guan, "A review of colloid transport in fractured rocks," Journal of Mountain Science **9**, 770–787 (2012).

[5] C. Hilgers and J. L. Urai, "Experimental study of syntaxial vein growth during lateral fluid flow in transmitted light: first results," Journal of Structural Geology **24**, 1029–1043 (2002).

[6] E. Dressaire and A. Sauret, "Clogging of microfluidic systems," Soft Matter **13**, 37–48 (2017).

[7] B. Dersoir, M. R. de Saint Vincent, M. Abkarian, and H. Tabuteau, "Clogging of a single pore by colloidal particles," Microfluidics and Nanofluidics **19**, 953–961 (2015).

[8] H. M. Wyss, D. L. Blair, J. F. Morris, H. A. Stone, and D. A. Weitz, "Mechanism for clogging of microchannels," Physical Review E **74** (2006), 10.1103/PhysRevE.74.061402.

[9] P. Bacchin, A. Marty, P. Duru, M. Meireles, and P. Aimar, "Colloidal surface interactions and membrane fouling: Investigations at pore scale," Advances in Colloid and Interface Science **164**, 2–11 (2011).

[10] P. Duru and Y. Hallez, "A Three-Step Scenario Involved in Particle Capture on a Pore Edge," Langmuir **31**, 8310–8317 (2015).

[11] M. Robert de Saint Vincent, M. Abkarian, and H. Tabuteau, "Dynamics of colloid accumulation under flow over porous obstacles," Soft Matter **12**, 1041–1050 (2016).

[12] B. Dersoir, A. B. Schofield, and H. Tabuteau, "Clogging transition induced by self filtration in a slit pore," Soft Matter **13**, 2054–2066 (2017).

[13] C. M. Cejas, F. Monti, M. Truchet, J.-P. Burnouf, and P. Tabeling, "Particle Deposition Kinetics of Colloidal Suspensions in Microchannels at High Ionic Strength," Langmuir **33**, 6471–6480 (2017).

[14] Y. Kim, K. H. Ahn, and S. J. Lee, "Clogging mechanism of poly(styrene) particles in the flow through a single micro-pore," Journal of Membrane Science **534**, 25–32 (2017).

[15] T. v. d. Laar, S. t. Klooster, K. Schron, and J. Sprakel, "Transition-state theory predicts clogging at the microscale," Scientific Reports **6** (2016), 10.1038/srep28450.

[16] Z. B. Sendekie and P. Bacchin, "Colloidal Jamming Dynamics in Microchannel Bottlenecks," Langmuir **32**, 1478–1488 (2016).

[17] C. Ghidaglia, L. de Arcangelis, J. Hinch, and l. Guazzelli, "Transition in particle capture in deep bed filtration," Physical Review E **53**, R3028 (1996).

[18] R. Narayan, J. R. Coury, J. H. Masliyah, and M. R. Gray, "Particle capture and plugging in packed-bed reactors," Industrial & engineering chemistry research **36**, 4620–4627 (1997).
[19] S. Hong, R. S. Faibish, and M. Elimielech, "Kinetics of Permeate Flux Decline in Crossflow Membrane Filtration of Colloidal Suspensions," Journal of Colloid ans Interface Science **196**, 267–277 (1997).
[20] M. Hieke, J. Ruland, H. Anlauf, and H. Nirschl, "Analysis of the Porosity of Filter Cakes Obtained by Filtration of Colloidal Suspensions," Chemical Engineering & Technology **32**, 1095–1101 (2009).
[21] G. A. Voth, A. La Porta, A. M. Crawford, J. Alexander, and E. Bodenschatz, "Measurement of particle accelerations in fully developed turbulence," Journal of Fluid Mechanics **469** (2002), 10.1017/S0022112002001842.
[22] R. B. Bird, "Transport phenomena," Applied Mechanics Reviews **55**, R1–R4 (2002).
[23] H. Bruus, *Theoretical microfluidics* (Oxford university press Oxford, 2007).
[24] E. L. Cussler, *Diffusion: Mass Transfer in Fluid Systems* (Cambridge University Press, 2009) google-Books-ID: dq6LdJyN8ScC.